Bull. Mater. Sci., Vol. 12, Nos 3 & 4, September 1989, pp. 325–340. © Printed in India.

Physical metallurgy of aluminium–lithium alloys

G J KULKARNI, D BANERJEE* and T R RAMACHANDRAN

Department of Metallurgical Engineering, Indian Institute of Technology, Kanpur 208 016, India
*Defence Metallurgical Research Laboratory, PO Kanchanbagh, Hyderabad 500 258, India

Abstract. The addition of lithium to aluminium reduces the density and increases the elastic modulus; precipitation of the metastable $\delta'(Al_3Li)$ phase from supersaturated Al–Li solid solution leads to appreciable increase in strength. The enhanced values for specific modulus and specific strength favour the use of the Al–Li alloys as structural materials for aerospace applications. However the binary alloys suffer from problems of poor ductility and toughness associated with strain localisation (resulting from the ease with which δ' particles are sheared during deformation), the presence of δ'-free zones near grain boundaries and the heterogeneous nucleation of the equilibrium δ phase on the grain boundaries. These problems have been overcome by the development of ternary and quaternary alloys containing copper and magnesium. A small amount (~0·1%) of zirconium is added to these alloys to improve the recrystallisation characteristics. The properties of alloys developed for commercial exploitation are briefly discussed. An overview of the physical metallurgy of the Al–Li alloys is presented with emphasis on the following features: (i) phase equilibria and precipitation reactions in Al–Li, Al–Cu–Mg, Al–Cu–Li and Al–Mg–Li systems and extension of these results to Al–Li–Cu–Mg alloys, (ii) insoluble particles and their effect on precipitation in the alloys, (iii) microstructural studies on Al–2·3%Li–1·2%Cu–0·7%Mg–0·12%Zr alloy, (iv) lithium depletion during solution treatment, (v) coarsening of δ' particles and development of precipitate-free zones near grain boundaries and (vi) microanalysis of the lithium containing phases.

Keywords. Aluminium–lithium alloys; phase equilibria; microstructure; solute depletion; coarsening; PFZ; microanalysis.

1. Introduction

The ever increasing need for economy of aircraft operation has resulted in a strong competition between conventional high strength aluminium alloys (7XXX series) and lighter but more rigid materials such as epoxy-based carbon fibre composites. It has been projected that the use of aluminium in aircraft structures would diminish progressively with composites and titanium alloys occupying more prominent positions (Quist *et al* 1984). However, the significant advance made in the development of aluminium–lithium alloys has, to a large extent, tilted the balance in favour of aluminium. The addition of lithium to aluminium reduces the density (~3% decrease for each wt.% of lithium) and increases the modulus (~6% increase per wt.% of lithium) (Starke *et al* 1981; Sankaran and Grant 1981). The Al–Li alloys are precipitation-hardenable, the metastable δ' phase formed during the ageing of supersaturated solid solution contributing to a large increase in strength (Noble and Thompson 1971). Consequently the substitution of conventional alloys of the 2XXX and 7XXX series by those containing lithium is expected to bring about a reduction of 10% in the weight of the aircraft leading to an estimated 4% savings in the operating costs (Quist *et al* 1984).

A historical perspective on the development of Al–Li alloys is given by Balmuth and Schmidt (1981) and Quist *et al* (1984). Initial investigations, carried out in Germany in the 1920's, were confined to the addition of small amounts of lithium to Al–Cu alloys. The commercial alloy 2020 developed in the US in 1958 was used on the wing surface of the RA-5C Vigilante aircraft. The alloy 01420 (Al–Mg–Li) was introduced in the USSR in 1969. Because of low ductility and fracture toughness in the maximum strength temper, the alloy 2020 was withdrawn in 1974. Since then a large number of investigations have been carried out in France, UK and USA to obtain better properties; these have involved the addition of ternary and quaternary solute elements and resorting to conventional ingot metallurgy and powder metallurgy techniques. A number of alloys, containing Cu, Mg and Zr in addition to Li, have been developed and their properties have been examined. The results of several of these studies are summarised in the Proceedings of the three International Conferences on aluminium-lithium alloys (*Aluminium–lithium alloys* 1981, 1984, 1986). The alloys are now produced on a semi-commercial scale; for example two caster units producing 1500 kg each of these alloys were operational in the Voreppe Research Centre of Pechiney, France in 1984; a 6000 kg unit is expected to go into operation sometime this year at Issoire, Pechiney, France.

Two important factors contribute to the poor ductility of the alloys. The first one is associated with the presence of impurity elements such as sodium, potassium, sulphur and hydrogen. These can be removed by the addition of suitable fluxes or elements such as bismuth, silicon or iron and efficient degassing procedure (Starke *et al* 1981). The second factor is associated with microstructural effects. The shearable nature of the δ' particles results in strain localisation which in turn leads to premature failure. The presence of a lithium–depleted zone near the grain boundary and the precipitation of the equilibrium δ phase at the grain boundary also contribute to low ductility (Starke *et al* 1981; Vasudevan *et al* 1985). Planar slip (or strain localisation) can be minimised by the addition of alloying elements which contribute to solid solution strengthening, form fine dispersoid particles, coprecipitate with δ' or incorporate lithium to form ternary phases which influence the strength and suppress the $\delta' \rightarrow \delta$ transformation (Sanders and Starke 1984). Small additions of zirconium or manganese to aluminium alloys result in the formation of dispersoid particles which have a strong retarding influence on recrystallisation characteristics. Addition of copper and or magnesium leads to the formation of new precipitating phases; besides, these elements also reduce the solubility of lithium in aluminium thereby increasing the volume fraction of δ'. Rapid solidification followed by consolidation and hot working leads to refinement of grains and dispersoid particles and minimises segregation effects.

A number of reviews have appeared in the literature dealing with various aspects of aluminium–lithium alloys (de Jong 1984; Welpmann *et al* 1984; Gregson and Flower 1986; Flower and Gregson 1987; Lavernia and Grant 1987). An attempt is made in this presentation to summarise some important features of the Al–Li alloys – these include details of alloys developed for commercial exploitation, and results on phase equilibria, nature of insoluble particles, lithium depletion during solution treatment, development of precipitate-free zones (PFZ's), coarsening of the δ' particles and determination of chemical composition of the lithium-containing phases.

2. Alloys of commercial interest

In view of the importance of the aluminium-lithium alloys, a large number of investigations have been carried out in USA, UK and France in the last 8 to 10 years. The main aim of these studies is to find replacements for the commonly used alloys, such as 2014, 2024 and 7075, with about 10% decrease in density and at least 10% increase in elastic modulus. These advantages together with the high fatigue crack growth resistance of the Al–Li alloys should favour their use for aircraft structures. The chemical composition, physical and mechanical properties of the alloys of commercial interest are shown in table 1 (Bretz and Sawtell 1986; Meyer and Dubost

Table 1. Chemical composition and properties of important Al–Li alloys.

	Chemical composition (wt%)						
Alloy	Li	Cu	Mg	Zr	Fe	Si	Mn
8090-CP 271	2·2–2·7	1·0–1·6	0·6–1·3	0·04–0·16	0·3	0·2	0·1
Lital-A	2·5	1·3	0·7	0·12	0·2	0·12	
8091-Lital-B	2·6	1·9	0·9	0·12	0·2	0·1	
CP 276	1·9–2·6	2·5–3·3	0·2–0·8	0·04–0·16	0·03	0·02	0·1
2090-Alithalite	1·9–2·6	2·4–3·0	0·25	0·08–0·15	0·12	0·1	
2091-CP 274	1·7–2·3	1·8–2·5	1·1–1·9	0·04–0·16	0·3	0·2	0·1

Alloy, temper	Density (g/cm^3)	Modulus (GPa)	YS (MPa)	UTS (MPa)	Elongation (%)
8090–T4	2·52–2·54	81·2	255	395	15
–T351			200	305	15
–T6			380	500	10·5
–T651			375	480	13
Lital–A, T–6					
Transverse	2·54	78·5	375	470	5·5
Longitudinal		78·0	365	465	7·5
Lital-C					
Transverse			335	450	6
Longitudinal			300	440	9
Lital–B, T–6					
Transverse	2·55	78·5	400	490	8
Longitudinal			410	505	9
CP 276–T6	2·57–2·60	80·2	490–590	590–640	5
–T651			575–625	600–655	5
–T6511			565	625	5·5
2090–T8					
Longitudinal	2·59	78·6	510	558	7·9
2091–T651	2·57–2·59	78·8	430	480	12
2014–T651	2·80	72·4	414	483	13
7075–T6	2·80	71·0	503	572	11

1986; Peel *et al* 1986). The lithium composition of these alloys lies in the range 1·7–2·6%, the copper content 1–3% and magnesium 0·6–2·0%. A small amount of zirconium is added for grain size control and retarding recrystallisation. The commonly encountered impurities, iron and silicon, are kept to low levels, <0·2%, to minimise the formation of insoluble particles. The mechanical properties of the alloys in various tempers are compared with those of 2014 and 7075. The lithium containing alloys have the advantage of at least 8% reduced density and 8–12% increased modulus. A wealth of information on the fracture toughness, fatigue and corrosion behaviour of these alloys has been collected. Simultaneously, alloy development to find replacements for the alloys 2324, 7010 and 7150 is under progress.

3. Phase equilibria and precipitation studies

No detailed phase equilibria studies have been carried out on the quaternary system Al–Li–Cu–Mg. However precipitation studies on a limited number of quaternary alloys reveal that the phases observed are the same as those found in Al–Li, Al–Cu–Mg, Al–Li–Mg and Al–Li–Cu alloys. Some pertinent aspects of phase equilibria and precipitation reactions in these alloys are reviewed in this section.

Investigations on Al–Li alloys have been carried out using the techniques of X-ray diffraction (Silcock 1959–60), transmission electron microscopy (Noble and Thompson 1971; Williams and Edington 1974), thermal analysis (Nozato and Nakai 1977; Papazian *et al* 1986), electrical resistivity measurements (Costas and Marshall 1962; Ceresara *et al* 1977) and small angle X-ray scattering (Cocco *et al* 1977; Spooner *et al* 1986). The Al-rich end of the phase diagram is shown in figure 1a (Gregson and Flower 1986). The equilibrium phases are the aluminium-rich solid solution (*FCC*, $a \sim 0{\cdot}405$ nm) and δ AlLi (*BCC*, $a = 0{\cdot}638$ nm). A metastable phase δ' Al_3Li ($L1_2$ cubic $a = 0{\cdot}401$ nm) appears during the ageing of the supersaturated solid solution. There is some evidence that this phase separates out during the quenching from solution treatment temperature (Noble and Thompson 1971; Williams and Edington 1975). This phase is responsible for precipitation-hardening. δ' forms as spheres possessing a cube–cube orientation relationship with the matrix. The lithium-vacancy binding enthalpy is significant ($\sim 0{\cdot}25$ eV); this can cause an appreciable retardation in the annealing of quenched-in vacancies. The δ' phase has relatively small misfit with the aluminium matrix, typically $-0{\cdot}1\%$ and low surface energy, $<30\,mJ/m^2$ (Sainfort and Guyot 1986). It has, therefore, been suggested that the phase forms by homogeneous nucleation from the supersaturated solid solution. The relatively low lithium content of Al_3Li ($\sim 7{\cdot}9$ wt.%) ensures large volume fraction of the metastable phase in alloys containing 2–3% lithium. Recent theoretical calculations of the stable and metastable phases in the Al–Li system indicate a miscibility gap which is metastable with respect to both the α (Al-rich solid solution) $-\delta$ and $\alpha-\delta'$ equilibria (Sigli and Sanchez 1986). This implies that if the formation of δ' can be suppressed during quenching, the supersaturated solid solution can decompose to form GP zones, either by nucleation and growth or spinodal decomposition. However with the exception of results of differential scanning calorimetry (Papazian *et al* 1986), there is no other evidence to support the formation of GP zones in these alloys.

Isothermal sections of the Al–Cu–Mg system are shown in figure 1b (Gregson and Flower 1986). The equilibrium phases formed depend on the relative amounts of

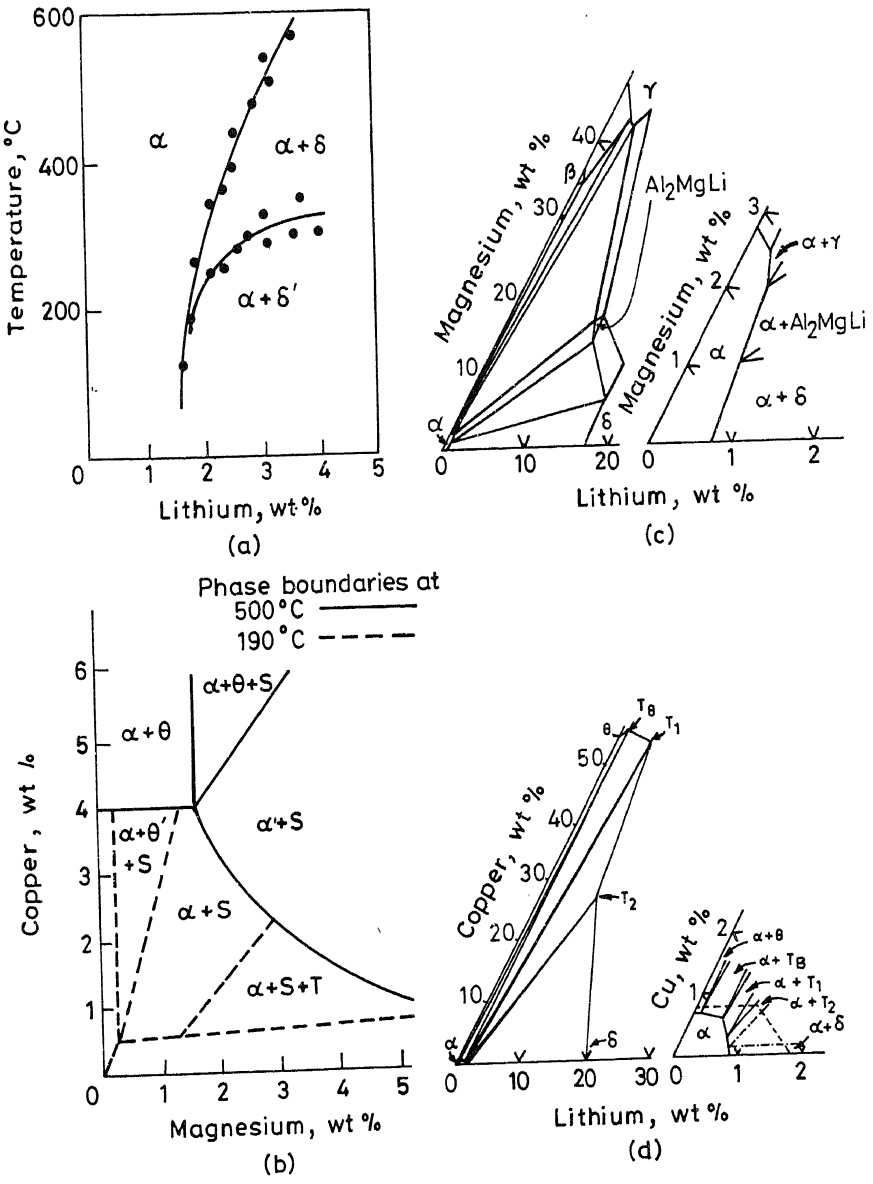

Figure 1. Phase equilibria in the systems (**a**) Al–Li, (**b**) Al–Cu–Mg, (**c**) Al–Li–Mg, and (**d**) Al–Li–Cu.

copper and magnesium. When the copper content is high, precipitation sequence is similar to that in binary Al–Cu alloys, viz. supersaturated solid solution → $GP1 \rightarrow \theta'' \rightarrow \theta' \rightarrow \theta$ ($CuAl_2$) (Silcock *et al* 1955–56). When the copper/magnesium ratio is less than 3:1, then the equilibrium phase S (Al_2CuMg) is formed preceded by the metastable S' phase (Silcock 1960–61). Precipitation of S occurs heterogeneously on dislocations. Quenched-in vacancies play an important role in this respect. When the magnesium content is high, the equilibrium phase T (Al_6CuMg_4) is formed. However this phase is not likely to appear in the alloys of interest to us.

The aluminium-rich end of the Al–Li–Mg system is shown in figure 1c (Schurman and Geissler 1980). The high solubility of magnesium in aluminium is relatively unaffected by the presence of lithium. From the enlarged section of this system presented in the figure, it is clear that apart from the equilibrium phase δ (and the metastable δ' phase) the only other phase of interest is the T (Al_2MgLi, cubic $a \simeq 2{\cdot}0$ nm) phase. These particles are formed as coarse dispersions and have little influence on the mechanical properties. On the other hand, the presence of δ' free zones near the particles (Flower and Gregson 1987) may adversely affect the ductility of the alloys. If the formation of the T phase can be prevented, a significant improvement in the properties of the alloys can be achieved. The alloy 01420 developed in USSR mainly contains magnesium (4·0–7·0%) and lithium (1·5–2·6%). Magnesium contributes to strength via solid solution hardening, reduction in lithium solubility and possibly by incorporation in the δ' itself (Baumann and Williams 1984; Dinsdale *et al* 1981; Harris *et al* 1984).

The isothermal section of the Al–Li–Cu system is shown in figure 1d (Hardy and Silcock 1955–56). The process of precipitation in copper-rich alloys is similar to that in binary Al–Cu alloys i.e. the formation of *GP*1, θ'', θ' and θ phases. However the presence of small amounts of lithium modify the orientation relation and structure of the homogeneously nucleated zones (Noble *et al* 1970) and the enhancement of precipitation of θ' at the expense of θ'' (Silcock 1959–60). There is some controversy about the effect of copper on the modification of the δ' solvus. Hardy and Silcock (1955–56) report a decrease in solubility of lithium in aluminium while Baumann and Williams (1984) point out that the solubility is unaffected. The equilibrium phases shown in figure 1d for compositions of interest are T_1, T_2 and T_B. The phase T_1 (Al_2CuLi, hexagonal) forms heterogeneously on dislocations and subgrain boundaries and high densities of this precipitate inhibit the growth of δ'. The phase $T_2(Al_6CuLi_3)$ is shown to display icosahedral symmetry (Crooks and Starke 1984; Loisseau and Lapasset 1986; Ball and Lloyd 1985; Ball and Lagacé 1986; Bartges *et al* 1987) and is commonly nucleated on grain boundaries. Recent investigations on Al–Li–Cu alloys show the existence of phases T_1', T_2' and T_B' which are precursors to the equilibrium phases (Suzuki *et al* 1982; Rioja and Ludwiczak 1986). T_1 is the most important of these phases as far as improvement of mechanical properties of the Al–Li–Cu–Mg alloys are concerned.

The addition of small amounts of Mn, Zr, Cr etc. is found to have a beneficial effect on the recrystallisation characteristics of aluminium alloys. Zirconium is particularly useful in this regard. It refines the as-cast grain structure and exerts a retarding influence on the recrystallisation associated with the formation of the metastable Al_3Zr ($L1_2$, $a \sim 0{\cdot}405$ nm) phase. Zirconium addition to Al–Li–Cu–Mg alloys does not affect the phase equilibria and precipitation sequence except for the introduction of the metastable Al_3Zr phase which may have an envelope of Al_3Li. This aspect is discussed in detail later. Addition of manganese leads to the formation of the equilibrium Al_6Mn. Precipitate-free zones are found around these particles indicating that this phase may heterogeneously nucleate δ. Studies show that the presence of δ has a deleterious effect on the corrosion resistance of aluminium-lithium alloys. Manganese does not appear to be a suitable addition to these alloys since the effect on slip homogenisation is marginal and it does not prevent strain localisation in PFZ's (Starke *et al* 1981).

Details of the phases appearing in the alloys of commercial interest are shown in

Table 2. Precipitating phases in aluminium–lithium alloys.

Phase	Crystal structure*	Orientation relationship	Remarks
AlLi (δ)	Cubic (NaTl) $a = 0{\cdot}638$	$(100)_p // (110)_{Al}$ $(011)_p // (\bar{1}11)_{Al}$ $(0\bar{1}1)_p // (1\bar{1}2)_{Al}$ Habit plane $(\bar{1}\bar{1}1)$	Equilibrium phase in the form of plates; addition of Cu or Mg does not affect the lattice parameter
Al_3Li (δ')	Cubic (Ll_2) $a = 0{\cdot}401$	Cube–cube	Metastable, coherent and ordered phase; spherical shape; lattice parameter varies slightly with Cu or Mg addition
Al_2CuLi(T_1)	Hexagonal, $a = 0{\cdot}4965$ $c = 0{\cdot}9345$	$[11\bar{2}0]_p // [2\bar{1}\bar{1}]_{Al}$ $(0001)_p // (111)_{Al}$ $(10\bar{1}0)_p // (1\bar{1}0)_{Al}$ Habit plane (111)	Partly coherent; coprecipitates with δ' for low Cu/Li ratio (2·5Cu–2Li) at all temperatures; above 170°C for medium Cu:Li ratio (3·5Cu–1·5Li); for high Cu:Li ratio (e.g. alloy 2020) precipitation sequence follows that in Al–Cu system
Al_6CuLi_3(T_2)	Cubic, $a = 1{\cdot}3914$		Displays icosahedral symmetry
$Al_{15}Cu_8Li_2$(T_B)	Cubic (CaF_2) $a = 0{\cdot}583$	$(100)_p // (110)_{Al}$ $(001)_p // (001)_{Al}$	
T'	Tetragonal $a = 0{\cdot}575$ $c = 0{\cdot}608$	$(001)_p // (001)_{Al}$ $(100)_p // (110)_{Al}$ $(010)_p // (1\bar{1}0)_{Al}$	Atomic ratio of Cu to Al is found to be in the range 0·5 to 1·0
Al_2CuMg(S')	Orthorhombic $a = 0{\cdot}404$ $b = 0{\cdot}925$ $c = 0{\cdot}718$	$(100)_p // (100)_{Al}$ $(010)_p // (021)_{Al}$ $(001)_p // (012)_{Al}$	Semi-coherent; rods grow along $\langle 110 \rangle_{Al}$ which widen forming laths in $\{210\}_{Al}$
Al_2CuMg(S)	Orthorhombic $a = 0{\cdot}400$ $b = 0{\cdot}923$ $c = 0{\cdot}714$	Similar to S'	Forms by coherency loss of S' or by heterogeneous nucleation on grain boundaries; incoherent equilibrium phase
Al_2MgLi	Cubic $a \simeq 2{\cdot}00$	$(\bar{1}10)_p // (\bar{1}10)_{Al}$ $(110)_p // (111)_{Al}$	Growth direction $\langle 110 \rangle_{Al}$
AlLiSi	Cubic $a \sim 0{\cdot}594$		
Al_3Zr	Cubic (Ll_2) $a = 0{\cdot}405$	Cube–cube	Spherical, coherent and ordered dispersoid particles found in zirconium-containing alloys

*Lattice parameters a, b, c in nm

Table 3. Insolubles in aluminium–lithium alloys.

Phase	Crystal structure	Lattice parameter (nm)
Al_7Cu_2Fe	Tetragonal	$a = 0{\cdot}6336$, $c = 1{\cdot}487$
$Al_{23}CuFe_4$	Orthorhombic	$a = 0{\cdot}7664$, $b = 0{\cdot}6441$, $c = 0{\cdot}8778$
$Al_{20}Cu_2Mn_3$	Orthorhombic	$a = 2{\cdot}411$, $b = 1{\cdot}251$ $c = 0{\cdot}72$
Al_5FeSi*	Monoclinic	$a = 0{\cdot}612$, $b = 0{\cdot}612$, $c = 4{\cdot}15$, $\beta = 91°$
Al_8Fe_2Si*	Hexagonal	$a = 1{\cdot}23$, $c = 2{\cdot}63$
$Al_6(Cu, Fe, Mn)$	Orthorhombic	$a = 0{\cdot}646$, $b = 0{\cdot}746$ $c = 0{\cdot}879$
$Al_{12}(Fe, Mn)_3Si$*	Cubic; space group $Pm\,3$	$a = 1{\cdot}265$

*10 different Al–Fe–Si phases have been reported in the literature (P Skjerpe 1987 *Metall. Trans.* **A18** 189); one or more of these phases may appear in the commercial Al–Li alloys

table 2, with information on crystal structure, orientation relationship and other important characteristics. The phase AlLiSi included in the table, is formed in silicon-containing alloys (Champier and Samuel 1986).

An important fact to be considered while discussing phase equilibria is the presence of impurities, iron and silicon. They give rise to coarse intermetallic compounds (insolubles), about 1–10 μm in size which can affect the properties significantly. Details of these compounds are shown in table 3. It can be seen that some of these compounds contain copper, thereby affecting the amount of copper available for the formation of the T_1 or S phase. The intermetallic particles would affect the precipitation characteristics by offering sites for heterogeneous nucleation; e.g. δ can be formed on them at the expense of metastable δ'. The presence of a precipitate-free zone around these particles would adversely affect the ductility. Also coarse insoluble particles decrease the fracture toughness of these alloys. Rapid solidification techniques are preferred in this respect as they lead to refinement of size of the insolubles.

4. Microstructural studies

It is now well-established that the Al–Li–Cu–Mg–Zr alloys develop optimum properties after artificial ageing of the solution-treated alloy in the temperature range 160–190°C (White *et al* 1986; Welpmann *et al* 1986) and that the improved mechanical properties result from the precipitation of δ', S and T_1 phases. The results of electron optical studies on an Al-2·3%Li–1·2%Cu–0·7%Mg–0·12%Zr alloy are presented in this section.

Typical examples of insoluble particles found in this alloy are shown in figures 2a and b. Elongated particles are seen in the extruded alloy (figure 2a). Occasionally spherical particles are found (figure 2b). X-ray microanalysis of these spherical particles reveals the presence of aluminium and silicon. The elongated particles are found to contain iron and copper. Several insoluble particles containing iron show icosahedral symmetry. A typical five-fold symmetry pattern obtained from an insoluble particle is shown in figure 2c. Solution treatment of the alloy followed by natural ageing for

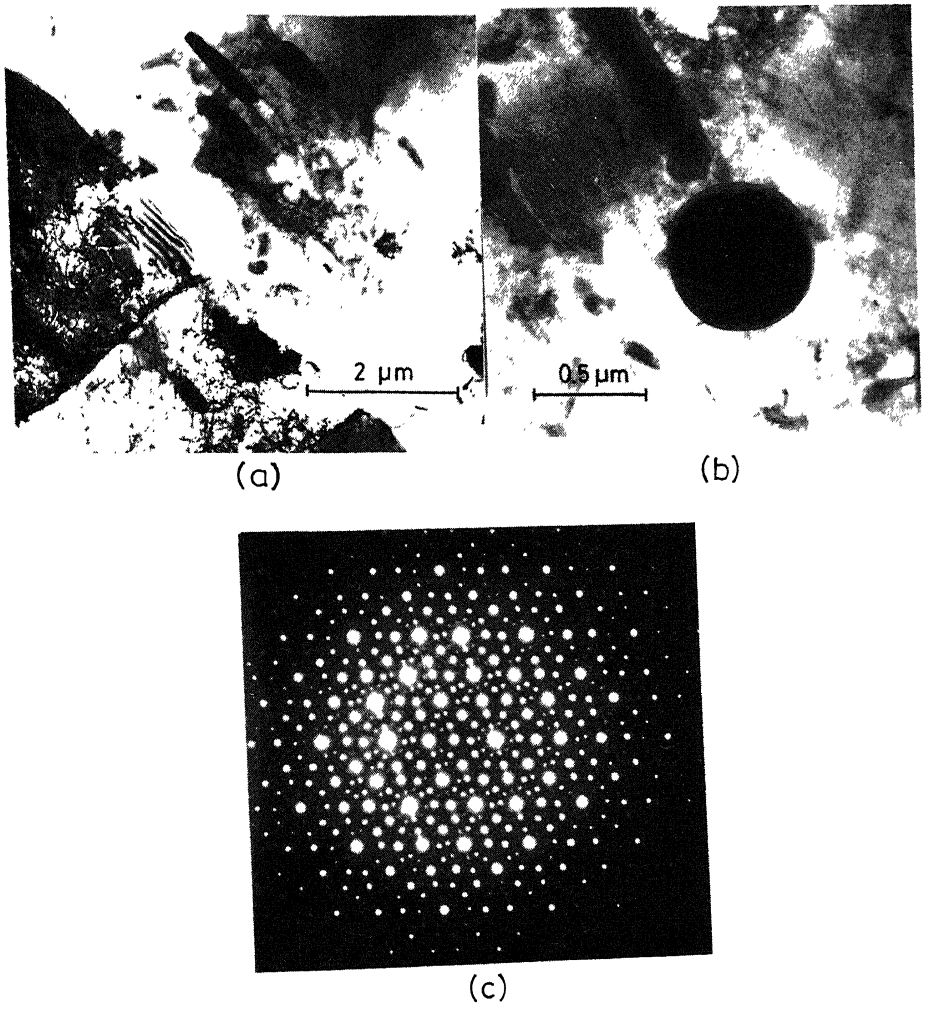

Figure 2. Insoluble particles in the Al–Li–Cu–Mg alloy: (**a**) in the extruded condition, (**b**) solution-treated and aged at 220°C for 24 h, (**c**) electron diffraction pattern from an insoluble particle showing five-fold symmetry.

a week results in the formation of dislocation loops due to condensation of quenched-in vacancies. Electron diffraction patterns reveal superlattice reflections due to δ'. The dislocation loops are stable even after annealing for 24 h at 160°C. This is illustrated in figure 3a in which a helical dislocation (formed by the condensation of vacancies on a screw dislocation) and two rhombus shaped loops are seen. In addition, there is a high density of a fine dispersion of δ' particles (size in the range 10–30 nm). Quenched-in defects play an important role in the nucleation of S and T_1 precipitates (Flower *et al* 1986; Gregson *et al* 1986). Ageing at 200°C for 24 h results in copious formation of S and T_1 phases (figure 3b). It is clear from this figure that the particles form along well defined crystallographic directions as indicated in table 2. There is profuse precipitation along grain boundaries which leads to reduced ductility. The nature of the precipitating phases is established by selected area electron diffraction.

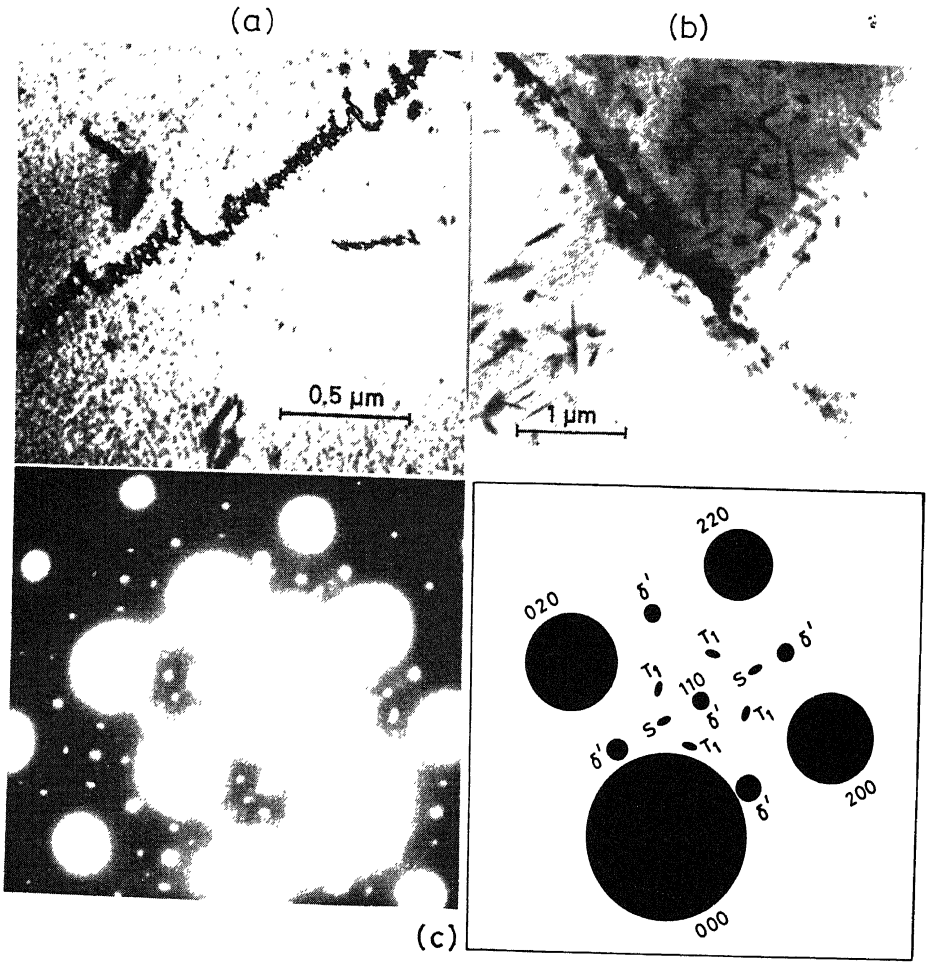

Figure 3. (**a**) Quenched-in vacancy defects and δ' particles in the Al–Li–Cu–Mg alloy, solution-treated and aged at 160°C for 24 h, (**b**) S and T_1 precipitation in the alloy after solution treatment and ageing at 200°C for 24 h; note the profuse grain boundary precipitation, (**c**) typical electron diffraction pattern after ageing at 220°C for 24 h and details of indexing.

A typical pattern corresponding to 24 h ageing at 220°C is shown in figure 3c. The matrix has the (001) orientation; the superlattice spots due to δ' are clearly seen. The four satellite spots surrounding the (110) δ' reflection arise from the presence of the T_1 phase and the other two spots from the S phase. The complete indexing of the relevant part of the diffraction pattern is shown in the figure.

5. Depletion of lithium during heat treatment

Heat treatment of aluminium–lithium alloys at elevated temperatures (solution treatment, thermomechanical treatment and superplastic forming) leads to preferential oxidation of lithium and magnesium and consequently to solute depleted layers near

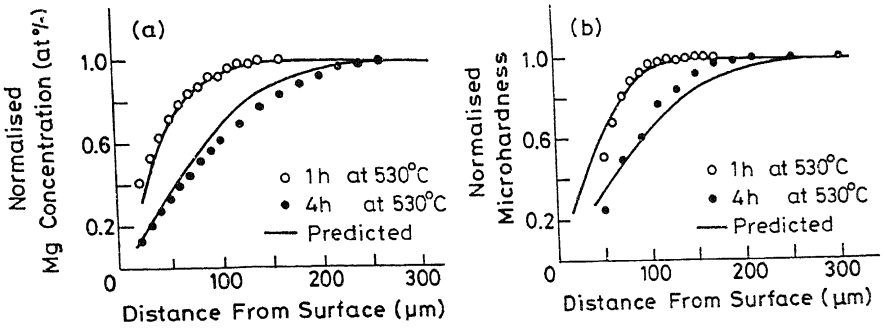

Figure 4. Depletion of solute as measured by (**a**) X-ray microanalysis for magnesium, (**b**) microhardness.

the surface. This can be inferred from the following values for the free energy of formation of the various oxides per mole of oxygen at 530°C (the commonly employed solution treatment temperature): −962 kJ for Al_2O_3, −1029 kJ for MgO and −1018 kJ for $LiAlO_2$ (Turkdogan 1980; Field *et al* 1984). As pointed out earlier, δ' contributes to the high strength of the alloy. Since depletion leads to progressively decreasing volume fractions of δ' in the surface layers, changes in the properties of the alloy are inevitable. A variety of techniques have been used to study solute-depletion; dilatometry and electrical resistivity measurements (Abd El-Salam *et al* 1983), eddy current conductivity (Wert and Ward 1985), microhardness measurements (Fox *et al* 1986a, b; Papazian *et al* 1986; Ahmad 1987), weight gain (Papazian *et al* 1986), nuclear reaction analysis (Papazian *et al* 1986) and X-ray microanalysis (Fox *et al* 1986a; Ahmad 1987). The oxidation products have been studied by X-ray diffraction and Auger electron spectroscopy (Ahmad 1987). The concentration profiles for lithium and magnesium obtained for the DTD XXXA (same as Lital A) alloy after heating at 530°C are shown in figure 4 (Fox *et al* 1986a). The concentration of magnesium has been established by wavelength dispersive analysis and that of lithium by microhardness measurements. Theoretically the concentration of the solute can be calculated from the solution to Fick's II law of diffusion:

$$C(x,t) = C_0 erf(x/2\sqrt{Dt}) \tag{1}$$

where C_0 is the concentration of the solute in the bulk material $C(x,t)$ is the concentration at a distance x from the surface, D is the diffusion coefficient and t is the heat treatment time. The good agreement between the theoretically calculated profile and the experimental results suggests that the oxidation process is controlled by solid state diffusion in the aluminium matrix. However, the results of another investigation (Field *et al* 1984) indicate interface control. It can be seen from figure 4 that the lithium- and magnesium-depleted layers are of the same size, 100–150 μm after 1 h treatment at 530°C. The recent results of Ahmad (1987) show negligible magnesium depletion. In general, it is found that the process of oxidation is accelerated by the addition of copper and magnesium while zirconium has little effect. The moisture content of the atmosphere is found to affect the oxidation rate adversely. Solute depletion is also found in samples treated in salt baths (e.g. a mixture of $NaNO_2$ and KNO_3). Removal of the solute-depleted layers is necessary for improving the mechanical properties.

6. Coarsening and precipitate-free zones

Prolonged ageing of the supersaturated solid solution of aluminium-lithium alloys leads to coarsening (Ostwald ripening) of the δ', S and T_1 phases; the coarse particles grow at the expense of the finer ones. The theory of coarsening of particles has been developed by Lifshitz and Slyozov (1959, 1961) and Wagner (1961). The mean radius $r(t)$ of the particles at a given time t during the coarsening process can be related to that at the beginning $r(0)$ by the expression,

$$r(t)^n - r(0)^n = Kt, \tag{2}$$

where n is a constant with values of 2, 3 or 4 depending on the rate controlling step (Lifshitz and Slyozov 1961; Wagner 1961; Ardell 1972). The constant K is defined by the expression,

$$K = (8\sigma C_{eq} D V_m^2)/(9RT), \tag{3}$$

where σ is the interfacial energy between the matrix and the precipitate, C_{eq} is the concentration of the solute in the matrix in equilibrium with the precipitate of infinite size, D is the diffusion coefficient of the solute and V_m is the molar volume of the precipitate. The coarsening theories predict a cut-off in the particle size distribution (PSD) curve at $r/\bar{r} = 1{\cdot}5$ where $\bar{r}$ is the mean particle radius. The PSD curve is asymmetric and is negatively skewed. The coarsening of the equilibrium δ phase at the grain boundary results in solute depletion in neighbouring regions leading to the formation of precipitate-free zones near grain boundaries. This region is vulnerable to strain localisation and hence contributes to reduced ductility and toughness. This aspect has recently been discussed by Vasudevan and Doherty (1987).

Most of the studies on coarsening and PFZ development have been carried out on binary alloys with lithium content varying from 2·4–4·5% and with small additions of manganese or zirconium (Noble and Thompson 1971; Williams and Edington 1975; Jensrud and Ryum 1984; Kulwicki and Sanders 1984; Jha *et al* 1987; Mahalingam *et al* 1987). Very few results are available for alloys containing copper and magnesium (Huang and Ardell 1986; Ahmad and Ericsson 1985, 1986). The results show that the coarsening of particles is controlled by diffusion in the matrix, i.e. $n = 3$; increasing lithium content and zirconium addition lead to enhanced kinetics; however, copper and magnesium additions have little effect. Experimentally determined PSD differs from the theoretically predicted one. Increasing the lithium content is shown to change the PSD from negatively skewed (at a volume fraction of 0·12) to positively skewed (at a volume fraction of 0·55) (Mahalingam *et al* 1987). The formation of Al_3Li on Al_3Zr particles gives rise to a bimodal PSD and accelerates the coarsening process. Increase in the volume fraction of δ' tends to make several particles nonspherical possibly due to coalescence. The coarsening data are used to obtain values for diffusion coefficient and interfacial energy which are in good agreement with those reported in the literature. The diameter of the hexagonal plate-shaped T_1 particles is found to increase linearly with the cube root of time, but Ostwald ripening is unlikely to be the coarsening mechanism, since the volume fraction increases with time (Huang and Ardell 1986). The value of the diffusion coefficient deduced from coarsening of S' is about 60–120 times smaller than that for diffusion of copper and magnesium in Al–Cu

and Al–Mg alloys; this is ascribed to the strong interaction between lithium atoms and vacancies (Ahmad and Ericsson 1985). The width of PFZ is found to increase with square root of time and with increasing lithium content and zirconium additions. The activation energy for the growth of PFZ is found to be 144 kJ/mol, comparable to that for diffusion of lithium in aluminium. In view of the importance of the quaternary alloys and the limited amount of studies of coarsening and development of PFZ, more work is clearly desirable in this area.

7. Microanalysis of lithium–containing phases

The determination of the chemical composition of the lithium-containing phases and variation of lithium in the aluminium matrix are expected to throw light on the following features: the stoichiometry of δ and δ' phases, lithium-depletion in the PFZ and derivation of diffusion parameters, amount of lithium available for solid solution hardening and for the formation of binary and ternary phases. These studies require the detection of small amounts of lithium with high spatial resolution (better than 10 nm). The most commonly employed method for the determination of chemical composition with high spatial resolution is X-ray microanalysis in which the intensities of the X-ray peaks from various elements are compared and, if necessary, corrections are applied for X-ray absorption and fluorescence. This technique is not suitable for the analysis of lithium for the following reasons (Sung *et al* 1986; Ball and Lagacé 1986): (i) the fluorescent yield for LiK X-ray is negligible ($<10^{-5}$); LiK X-ray is soft (energy $\sim$52 eV) and is therefore easily absorbed; if a crystal spectrometer were to be used for the analysis of the soft X-ray, an analysing crystal with a d spacing of $\sim$23 nm would be required, (ii) quantitative X-ray microanalysis for low levels of magnesium in aluminium alloys is susceptible to large errors because of the proximity of MgK(1·254 keV) and AlK (1·487 keV) peaks and (iii) quantitative microanalysis in alloys containing copper is complicated by the tendency of copper to redeposit on the surface of the specimen during electropolishing (van Heimendahl and Puppel 1982) giving rise to spuriously high values for copper concentration. Electron energy loss spectroscopy is ideally suited for the study of light elements. The chemical composition of the sample can be obtained from plasmon loss measurements or ionisation edge studies. The former involves the measurement of the shift of the first plasmon peak as a function of the solute content. Williams and Edington (1974) have shown that this technique can be used for the determination of small changes in lithium content on a scale 10 nm. Sainfort and Guyot (1985) carried out plasmon loss measurements in pure aluminium, solid solution of lithium in aluminium and δ' and determined the concentration dependence of the shift of the plasmon loss peak. In general EELS studies require very thin specimens; Malis (1986) used ultramicrotomed specimens for ionisation edge studies. Chan and Williams (1985) used this technique to determine the composition of δ' to be $Al_{3\cdot60\pm0\cdot64}Li$. The large error bands are associated with problems of background subtraction procedure and uncertainties in the ionisation cross section values. Higher order Laue zone (HOLZ) lines found in convergent beam diffraction patterns have also been used to study variations in lattice parameters and hence in chemical composition (Sung *et al* 1986).

It has already been pointed out that Al_3Li can nucleate on Al_3Zr particles. This

gives rise to the 'do nut' or 'bull's eye' structure. The zirconium-containing particles have high antiphase boundary energy (447 mJ/m^2) in contrast to that of 180 mJ/m^2 of Al_3Li (Flower and Gregson 1987). The difficulty of shearing the former leads to homogenisation of the slip. There is growing interest in the study of the distribution of lithium and group IV-A transition elements (Zr, Ti, Hf) in the composite Al_3Li–Al_3Zr phase. An interesting point in this regard is that Al_3Ti, which is normally tetragonal, is observed to be stabilised as the ordered $L1_2$ phase in the presence of lithium (Gayle *et al* 1987). The composition of the composite particles has been determined by a number of techniques: (i) electron energy loss spectroscopy, (ii) comparing the observed dark field images with those computed, taking into account the diffraction conditions, various lithium/transition metal ratios and the radius of the core of the composite particle as a fraction of its overall radius (Gayle *et al* 1987) and (iii) atom probe field ion microscopy (Hono *et al* 1986; Sakurai *et al* 1986). There is a general agreement that at high temperature the composite particle contains about 5–10% lithium. However, conflicting results are reported about possible changes in composition during ageing; the dark field images suggest no change while atom probe studies indicate an increase in the composition of the transition element. The incorporation of lithium in the transition metal-containing phase is important as far as precipitation reactions and coarsening processes are concerned and this is an area where further investigations are required.

8. Concluding remarks

The results of a large number of investigations clearly show that the Al–Li–Cu–Mg–Zr alloys are capable of developing strength properties comparable to the presently used 2XXX and 7XXX aluminium alloys, but with lower density and increased elastic modulus. However, a number of features are to be investigated further to improve our understanding of these alloys. Among them, the following need serious consideration: (i) phase equilibria studies in the complex alloys, (ii) at least a semi-quantitative assessment of the distribution of copper, and possibly of lithium, in the insolubles so that the amount of these solutes available for the formation of useful precipitates can be estimated, (iii) microstructural studies related to the distribution of lithium in δ', δ and Al_3Zr (or any other transition metal) and quantitative estimates of the volume fraction of various precipitates, (iv) the extent of lithium and magnesium depletion in quaternary alloys, (v) coarsening of the precipitates and development of PFZ in the complex alloys to understand the effect of copper and magnesium and (vi) analytical electron microscopy of the various phases using X-ray microanalysis, electron energy loss spectroscopy and convergent beam diffraction.

Acknowledgements

This work is supported by the Department of Science and Technology, New Delhi under the project 'Microstructural Studies on Aluminium–Lithium–Copper–Magnesium Alloys'. The authors are grateful to Prof. P Rama Rao for his support and constant encouragement.

References

Aluminium–lithium alloys III, (eds) Baker C, Gregson P J, Harris S J and Peel C 1986 The Institute of Metals, London

Aluminum–lithium alloys (eds) Sanders T H and Starke E A 1981 TMS–AIME Warrendale, PA

Aluminum–lithium alloys II, (eds) Sanders T H and Starke E A 1984–AIME, Warrendale, PA

Abd El-Salam F, Eatah A I and Tawfik A 1983 *Phys. Status Solidi* (a) **75** 379

Ahmad M 1987 *Metall. Trans.* **A18** 635

Ahmad M and Ericsson T 1985 *Scr. Metall.* **19** 457

Ahmad M and Ericsson T 1986 *Aluminum–lithium alloys III* p. 509

Ardell A J 1972 *Acta Metall* **20** 61

Ball M D and Lloyd D J 1985 *Scr. Metall.* **19** 1065

Ball M D and Lagacé H 1986 *Aluminium–lithium alloys III* p 555

Balmuth E S and Schmidt R 1981 *Aluminum–lithium alloys* p 69

Bartges C, Tosten M H, Howell P R and Ryba E R 1987 *J. Mater. Sci.* **22** 1663

Baumann S F and Williams D B 1984 *Aluminum–lithium alloys II* p 17

Bretz P E and Sawtell R R 1986 *Aluminium–lithium alloys III* p 47

Ceresara S, Giarda A and Sanchez A 1977 *Philos. Mag.* **35** 97

Champier G and Samuel F H 1986 *Aluminium–lithium alloys III* p 131

Chan H M and Williams D B 1985 *Philos. Mag.* **B52** 1019

Cocco G, Fagherazzi C and Schiffini L 1977 *J. Appl. Cryst.* **10** 325

Costas L P and Marshall R P 1962 *Trans. AIME* **224** 970

Crooks R E and Starke E A 1984 *Metall. Trans.* **15A** 1367

de Jong H 1984 *Aluminium* **60** E587

Dinsdale K, Harris S J and Noble B 1981 *Aluminum–lithium alloys* p 101

Field D J, Scamans G M and Butler E P 1984 *Aluminum–lithium alloys* II p 657

Flower H M and Gregson P J 1987 *Mater. Sci. Technol.* **3** 81

Flower H M, Gregson P J, Tite C N J and Mukhopadhyaya A K 1986 *Aluminum alloys: Their physical and mechanical properties* (eds) Starke E A and Sanders T H, (Warley: Engineering Materials Advisory Service), Vol 2

Fox S, Flower H M and McDarmaid D S 1986a *Scr. Metall.* **20** 1986

Fox S, Flower H M and McDarmaid D S 1986b *Aluminium–lithium alloys III* p 263

Gayle F W, Levoy N F and VanderSande J B 1987 *J. Met.* **39(5)** 33

Gregson P J and Flower H M 1986 *Aluminium technology* '86 (ed.) T Sheppard (London: Institute of Metals) p 423

Gregson P J, Flower H M, Tite C N J and Mukhopadhyay A K 1986 *Mater. Sci. Technol.* **2** 349

Hardy H K and Silcock J M 1955–56 *J. Inst. Met.* **84** 423

Harris S J, Noble B and Dinsdale K 1984 *Aluminum–lithium alloys II* p 219

Hono K, Abe T, Hess D R, Pickering H W, Howell P R, Hasegawa Y, Sakurai T, Sano N and Hirano K 1986 *Aluminum alloys: Their physical and mechanical properties*, p 621

Huang J C and Ardell A J 1986 *Aluminium–lithium alloys III* p 455

Jensrud O and Ryum N 1984 *Mater. Sci. Eng.* **64** 229

Jha S C, Sanders T H and Dayananda M 1987 *Acta Metall.* **35** 473

Kulwicki J H and Sanders T H 1984 *Aluminum–lithium alloys II* p 31

Lavernia E J and Grant N J 1987 *J. Mater. Sci.* **22** 1521

Lifshitz I M and Slyozov V V 1959 *Soviet Physics JETP*, **35(8)** 331

Lifshitz I M and Slyozov V V 1961 *J. Phys. Chem. Solids* **19** 35

Loisseau A and Lapasset G 1986 *J. Phys.* (*Paris*) **47** C3–331

Mahalingam K, Gu B P, Liedl G L and Sanders T H 1987 *Acta Metall.* **35** 483

Malis T 1986 *Aluminium–lithium alloys III* p 347

Meyer P and Dubost B 1986 *Aluminium–lithium alloys III* p 37

Noble B, McLaughlin I R and Thompson G 1970 *Acta Metall.* **18** 339

Noble B and Thompson G E 1971 *Met. Sci. J.* **5** 114

Nozato R and Nakai G R 1977 *Trans. Jpn. Inst. Metals* **18** 678

Papazian J M, Schulte R L and Adler P N 1986 *Metall. Trans.* **A17** 635

Peel C J, Evans B and McDarmaid D 1986 *Aluminium–lithium alloys III* p 26

Quist W E, Narayanan G H and Wingert A L 1984 *Aluminium–lithium alloys II* p 313
Rioja R A and Ludwiczak E A 1986 *Aluminium–lithium alloys III* p 471
Sainfort P and Guyot P 1985 *Philos. Mag.* **A51** 575
Sainfort P and Guyot P 1986 *Aluminium–lithium alloys III* p 420
Sakurai T, Kobayashi A, Hasegawa Y, Sakai A and Pickering H W 1986 *Scr. Metall.* **20** 1131
Sanders T H, Ludwiczak E A and Sawtell R R 1980 *Mater. Sci. Eng.* **43** 247
Sanders T H and Starke E A 1984 *Aluminum–lithium alloys II* p 1
Sankaran K K and Grant N J 1981 *Aluminum–lithium alloys* p 205
Schurman and Geissler I K 1980 *Giessereiforschung* **32** 163
Sigli C and Sanchez J M 1986 *Acta Metall.* **34** 1021
Silcock J M, Heal T J and Hardy H K 1955–56 *J. Inst. Met.* **84** 23
Silcock J M 1959–60 *J. Inst. Met.* **88** 357
Silcock J M 1960–61 *J. Inst. Met.* **89** 203
Spooner S, Williams D B and Sung C M 1986 *Aluminium–lithium alloys III* p 329
Starke E A, Sanders T H and Palmer I G 1981 *J. Met.* **33(8)** 24
Sung C M, Chan H M and Williams D B 1986 *Aluminium–lithium alloys III* p 337
Suzuki H, Kanno M and Hayashi N 1982 *J. Jpn. Inst. Light Met.* **32** 88
Turkdogan T 1980 *Phys. Chem. High Temp. Technology* (New York, London: Academic Press)
van Heimendahl M and Puppel D 1982 *Micron* **13** 1
Vasudevan A K, Ludwiczak E A, Baumann S F, Doherty R D and Kersker M M 1985 *Mater. Sci. Eng.* **72** 125
Vasudevan A K and Doherty R D 1987 *Acta Metall.* **35** 1193
Wagner C 1961 *Z. Electrochem.* **65** 581
Welpmann K, Peters M and Sanders T H 1984 *Aluminium* **60** E641
Welpmann K, Peters M and Sanders T H 1986 *Aluminium–lithium alloys III* p 524
Wert J A and Ward A B 1985 *Scr. Metall.* **19** 367
White J, Miller W S, Palmer I G, Davis R and Saini T S 1986 *Aluminium–lithium alloys III* p 530
Williams D B and Edington J W 1974 *Philos. Mag.* **30** 1147
Williams D B and Edington J W 1975 *Met. Sci. J.* **9** 529